

Structural Effect of Amphiphilic Crown Ether Azoprobes on Alkali Metal Ion Recognition and Aggregation Behavior in Water

Fuyuki Sato, Miki Tsukano, Koki Sakamoto, Wakako Umemoto, Takeshi Hashimoto, and Takashi Hayashita*

Department of Chemistry, Faculty of Science and Technology, Sophia University, 7-1 Kioi-cho, Chiyoda-ku, Tokyo 102-8554

Received May 26, 2008; E-mail: ta-hayas@sophia.ac.jp

Amphiphilic azoprobes having a crown ether moiety (15C5–Azo–C*n*; $n = 4$, 6, 8, and 12 and 18C6–Azo–C*n*; $n = 4$, 6, and 8) were synthesized. We examined the effect of alkyl spacer length of the amphiphilic azoprobes on the spectral response to alkali metal ions in water by UV–vis spectral and ^{1}H NMR measurements. 15C5–Azo–C*n* exhibited self-assembly in response to K^+ selectively and the most selective response to K^+ was observed for an azoprobe possessing a hexyl spacer unit (15C5–Azo–C6). 15C5–Azo–C12 formed nano-size aggregates. 18C6–Azo–C*n* ($n = 6$ and 8) showed Cs^+ selectivity and its molecular aggregation behavior was similar to that of 15C5–Azo–C*n*.

Alkali metal ion recognition in water is an emerging topic of interest in analytical and biological chemistry. Although various efficient chemosensors that function as unimolecular sensors have been developed, most of them require precise design of the ion recognition sites to achieve sufficient selectivity and sensitivity for alkali metal ions in water. Meanwhile, new approaches for the versatile design of recognition sites, which are based on supramolecular chemistry, have been attracting much attention. Recently, we have endeavored to combine supramolecular chemistry and self-assembly to fabricate supramolecular sensors that exceed the sensitivity and selectivity of unimolecular sensors and mimic the functions of biomolecules. Supramolecular sensors for alkali metal ions utilize various types of metal-binding induced aggregates for signal transduction, including fluorescent bis-15-crown-5 derivatives,[1] gold nanoparticles and quantum dots,[2] oligonucleotides,[3] and cyclodextrin complexes.[4] It is well known that amphiphiles are water-soluble and their critical micelle concentration (cmc) and aggregate structures are dependent on their structure and alkyl chain length, i.e., hydrophilicity–lipophilicity balance (HLB).[5] Therefore, supramolecular sensors possessing an amphiphilic skeleton are considered to be useful for the versatile design of chemosensors that function in water, and recognition ability can be tuned easily by controlling the strength of aggregation.

Here, we report cationic azo-amphiphiles, 15C5–Azo–C*n* and 18C6–Azo–C*n*, possessing 15-crown-5 and 18-crown-6 moieties, respectively, as the alkali metal ion recognition site; a phenylazo group for signal transduction; and a quaternary ammonium unit with different lengths of alkyl spacers to induce the amphiphilic nature. We have recently reported the K^+ recognition selectivity of 15C5–Azo–C*n* ($n = 2$, 4, and 6) in water by forming H-aggregate dimers triggered by K^+ binding based upon exciton interaction of the phenylazo groups in the azoprobes.[6] Among these azoprobes, 15C5–Azo–C6 exhibited the best performance. In this study, alkyl spacer lengths were varied from butyl to dodecyl to estimate the most suitable structure to recognize target ion species in water. As a result, 15C5–Azo–C6 exhibited the best performance, and azoprobes having long alkyl spacers showed decreased K^+ binding ability due to strong aggregation. In particular, 15C5–Azo–C12 formed nano size aggregates to exhibit the lowest K^+ selectivity. In addition, the effect of crown ether ring size on metal ion selectivity was examined. While 18-crown-6 is known to bind with K^+, Xia et al. have reported an 18-crown-6 fluoroionophore that selectively binds Cs^+ by forming a 2:2 sandwich complex.[7] In this study, we have synthesized amphiphilic azoprobes possessing 18-crown-6 as the ion recognition moiety (18C6–Azo–C*n*; $n = 4$, 6, and 8), and compared the ion recognition characteristics with those of 15C5–Azo–C*n* to clarify the ring size effect. These derivatives showed Cs^+ selectivity and similar aggregation behavior was obtained in comparison to 15C5–Azo–C*n*. 18C6–Azo–C6 and –C8 showed higher Cs^+/Na^+ selectivity than 18C6–Azo–C4.

Experimental

General. Aqueous sample solutions were prepared with a Millipore milli-Q water system (electric conductivity: 18.2 $M\Omega\,cm^{-1}$). To retain the trans configuration of the azoprobes, all sample preparation steps were accomplished in the dark. All organic solvents and reagents were commercially available and used without further purification.

Apparatus. UV–vis absorption spectra were recorded on a V-560 (JASCO Co.) and a U-3000 (Hitachi High-Technologies Co.) spectrophotometer equipped with a Peltier thermocontroller with a 0.01-cm quartz cell at 298 K. ^{1}H NMR spectra were measured with a Lambda500 (JEOL Ltd.; 500 MHz) at 300 K. Nonlinear least-squares fitting was done with KaleidaGraph (Synergy Software).

Synthesis of 15C5–Azo–C*n* and 18C6–Azo–C*n*. Amphiphilic crown ether azoprobes (15C5–Azo–C*n* ($n = 4$, 6, 8, and 12) and 18C6–Azo–C*n* ($n = 4$, 6, and 8)) were synthesized, as shown in Scheme 1. The preparation of 15C5–Azo–C*n* started from 4′-ami-

Published on the web December 12, 2008; doi:10.1246/bcsj.81.1589

nobenzo-15-crown-5-ether (**4**), followed by azo coupling with phenol (**5a**). Then, 1,*n*-dibromoalkane was coupled by Williamson ether synthesis. Finally, quaternalization with trimethylamine gave the desired compounds. For the preparation of 18C6–Azo–C*n*, nitration of benzo-18-crown-6 (**1**) was carried out in dichloromethane/acetic acid solution containing nitric acid to afford 4′-nitrobenzo-18-crown-6 (**2**), and 4′-aminobenzo-18-crown-6 hydrochloride (**3**) was prepared by reducing **2** with hydrazine monohydrate in the presence of 10% Pd/C.[8] The remaining steps for 18C6–Azo–C*n* syntheses were almost the same as those for 15C5–Azo–C*n*. Their structures were fully confirmed by ^{1}H NMR, mass, and elemental analyses (see Supporting Information).

Results and Discussion

Effect of Alkyl Spacer Length. In a previous report, we have shown that 15C5–Azo–C*n* ($n = 2$, 4, and 6) exhibited self-assembly in response to alkali metal ions in water, and the highest response to K^+ was noted for 15C5–Azo–C6 possessing a hexyl spacer unit, indicating that the longer alkyl spacer stabilized the H-aggregate dimer formation upon binding with K^+. In this study, we additionally prepared azoprobes having longer alkyl spacers ($n = 8$ and 12) because we are interested in how longer alkyl spacers affect the response efficiency and selectivity of 15C5–Azo–C*n*.

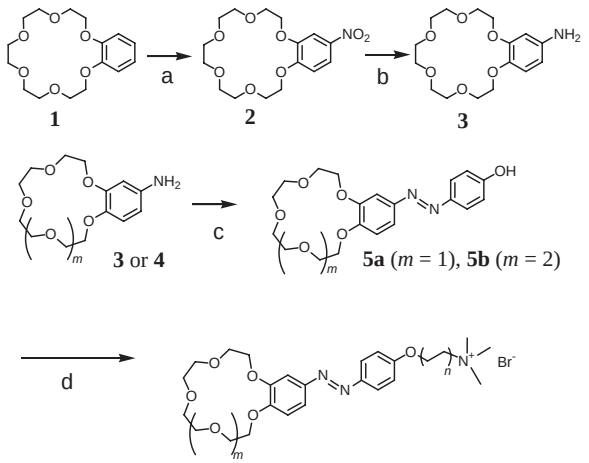

Scheme 1. Synthesis of 15C5–Azo–C*n* and 18C6–Azo–C*n*. (a) HNO_3, H_2SO_4, CH_3COOH, CH_2Cl_2; (b) Pd/C, $N_2H_4 \cdot H_2O$, THF; (c) $NaNO_2$, HCl, $H_2O \rightarrow C_6H_5OH$, NaOH; (d) K_2CO_3, $Br(C_2H_4)_nBr$, $(C_4H_9)_4NI$, THF $\rightarrow$ $N(CH_3)_3$, THF. For 15C5–Azo–C*n* ($m = 1$), $n = 4$, 6, 8, and 12. For 18C6–Azo–C*n* ($m = 2$), $n = 4$, 6, and 8.

Figure 1a shows the UV–vis absorption spectra of 15C5–Azo–C6 (3.0 mM) in water containing 400 mM tetramethylammonium chloride (TMACl), NaCl, or KCl. The maximum wavelength can be assigned to the long axis polarized π–π^* transition band of the phenylazo group in the azoprobes.[9] As we have reported in a previous paper, 15C5–Azo–C6 exhibited no significant change in its UV–vis spectra in the presence of TMA^+ or Na^+. In contrast, a clear hypsochromic shift of the π–π^* transition band of the azoprobe was observed in the presence of K^+. Based on the exciton theory,[10] this shift can be assigned to H-aggregate dimer formation triggered by K^+ binding. Although the binding ability of 15-crown-5 with K^+ in water is very weak ($<1.0\,M^{-1}$),[11] we assume that the amphiphilic nature of the azoprobe and the π–π^* stacking ability of the phenylazo units stabilize the H-aggregate dimer formation with K^+ in water. We have already shown a similar UV–vis spectral change for bis-15-crown-5 ether azoprobe by forming an intramolecular sandwich complex with K^+ in acetonitrile, which supports a similar type of H-aggregate dimer formation for 15C5–Azo–C6 in water.[12] Figure 1b shows the effect of alkyl spacer length on the response selectivity. The ratio of absorbance at 370 nm to that at 420 nm (A_{370}/A_{420}) is plotted against the ionic radius of alkali metal ions (Li^+, Na^+, K^+, Rb^+, and Cs^+). The results clearly show K^+ selectivity of all the azoprobes, and the highest response was obtained for 15C5–Azo–C6.

To confirm the structural details of H-aggregate formation, ^{1}H NMR spectra of the phenyl protons of 15C5–Azo–C*n* were compared (Figure 2). Compared with proton signals measured in the presence of TMACl for 15C5–Azo–C*n* ($n = 4$, 6, and 8), no chemical shift was observed after the addition of 400 mM NaCl. In contrast, distinct upfield shifts of the proton signals were observed after the addition of KCl, particularly for 15C5–Azo–C6. The results reveal the ring-current effect due to the formation of H-aggregates triggered by binding with

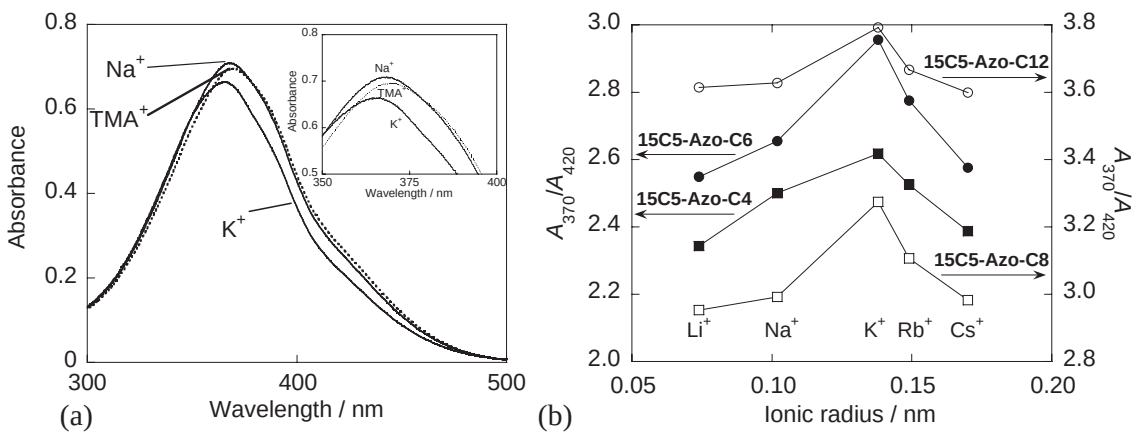

Figure 1. (a) UV–vis spectral changes of 15C5–Azo–C6 on addition of 400 mM NaCl, KCl, and TMACl. (b) Response of 15C5–Azo–C*n* ($n = 4$, 6, 8, and 12) to each alkali metal ion. [MCl] = 400 mM ($M^+ = Li^+$, Na^+, K^+, Rb^+, and Cs^+), [15C5–Azo–C*n*] = 3.0 mM.

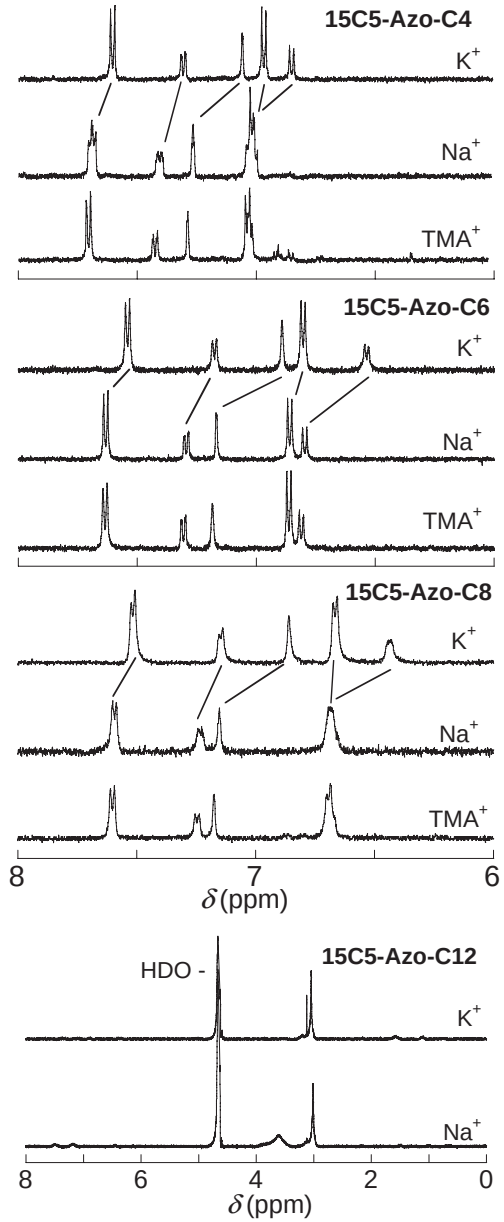

Figure 2. ^{1}H NMR spectra of phenyl protons of 15C5–Azo–C*n* ($n = 4$, 6, 8, and 12) in D_2O at 300 K. [15C5–Azo–C*n*] = 3.0 mM, [MCl] = 400 mM (M = K^+, Na^+, and TMA^+).

K^+. This binding mechanism is consistent with the hypsochromic shift of the π–π^* transition band of the azo moiety in the UV–vis absorption spectra. In addition, each peak was shifted upfield as the alkyl spacer length increased under the same salt condition, indicating that aggregation was promoted with the increase in alkyl spacer length.

Interestingly, except for the signal of the quaternary ammonium group the proton signals of 15C5–Azo–C12 were too broad to observe after the addition of K^+, whereas severely broadened signals were observed after the addition of Na^+. This signal broadening may be due to the decline in molecular motion with aggregate formation.[12] Kunitake and Okahata compared the synthetic bilayer membrane of didodecyldimethylammonium bromide (DDAB) with the spherical micelle of cetyltrimethylammonium bromide (CTAB) using ^{1}H NMR measurement.[13] CTAB showed a definite signal assignable to the quaternary ammonium group and the cetyl group above cmc, while DDAB showed considerably broadened signals due to the formation of multilayered vesicles and lamellae. In our study, the distinct signal of the quaternary ammonium group indicates that the positioning at the quaternary ammonium group is oriented outside the aggregate where methyl units are relatively free to move, and other moieties, including crown ether, phenylazo, and alkyl spacer, are located inside the aggregate. Thus, more closely packed aggregates may be formed by K^+-binding. Although the detailed structure of 15C5–Azo–C12 aggregates is not clear at this stage, preliminary light-scattering experiments suggested that a smaller size distribution was observed upon addition of K^+ rather than of Na^+ (Supporting Information).

Effect of Crown Ether Ring Size on Response Selectivity. In Figure 3a are shown the UV–vis absorption spectra of 18C6–Azo–C6 (3.0 mM) in water containing 400 mM TMACl, NaCl, or CsCl. Similar to 15C5–Azo–C*n*, 18C6–Azo–C*n* exhibited no significant response in the presence of TMA^+ or Na^+. In contrast, a clear hypsochromic shift of the π–π^* transition band of the azoprobe was observed in the presence of Cs^+, indicating that the H-aggregate dimer formation of 18C6–Azo–C*n* was triggered by Cs^+ binding. The plots of A_{370}/A_{420} against the ionic radius of alkali metal ions are depicted in Figure 3b. Due to the large ring size of 18-crown-6 (0.26–0.32 nm) compared with that of 15-crown-5 (0.17–0.22 nm), the change in ion selectivity from K^+ to Cs^+ is evident for 18C6–Azo–C*n*. Interestingly, the response to Li^+ was noted to some extent for 18C6–Azo–C6 and 18C6–Azo–C8, although the reason is not clear, Kikuchi et al. reported the formation of the Li^+–H_2O–18-crown-6 complex in acetone/water mixture.[14] This type of complex formation may have some relationship with the response to Li^+. That the extent of peak shift for 18C6–Azo–C*n* was smaller than that for 15C5–Azo–C*n* is an indication of weaker dipole–dipole interaction, because the distance between phenylazo moieties on H-aggregate dimers should be longer due to the larger ionic radius of Cs^+ than that of K^+.

Figure 4 shows changes in the absorbance ratio (A_{370}/A_{420}) with the concentration of 15C5–Azo–C*n* or 18C6–Azo–C*n*. The deviation from linearity (A_{370}/A_{420} = ca. 2.3) indicates aggregate dimer formation. In the absence of salt, A_{370}/A_{420} showed almost linear up to 5 mM for the azoprobes having a butyl or hexyl spacer. As alkyl spacer length extended from octyl to dodecyl, the break point shifted to lower concentration for 15C5–Azo–C*n*. This indicates that aggregation was enhanced with the increase in alkyl spacer length. A similar behavior was noted for 18C6–Azo–C*n*.

Changes in A_{370}/A_{420} values and the maximum wavelength (λ_{max}) of 15C5–Azo–C*n* upon the addition of 400 mM KCl and of 18C6–Azo–C*n* upon the addition of 400 mM CsCl are summarized in Table 1. 15C5–Azo–C4 remained in the monomer state ($A_{370}/A_{420} = 2.3$), while 15C5–Azo–C6 partially formed aggregates ($A_{370}/A_{420} = 2.5$). For 15C5–Azo–C8 and 15C5–Azo–C12, λ_{max} values below 370 nm and large values of A_{370}/A_{420} upon the addition of TMA^+ indicate that these azoprobes formed H-aggregates without K^+ due to the hydro-

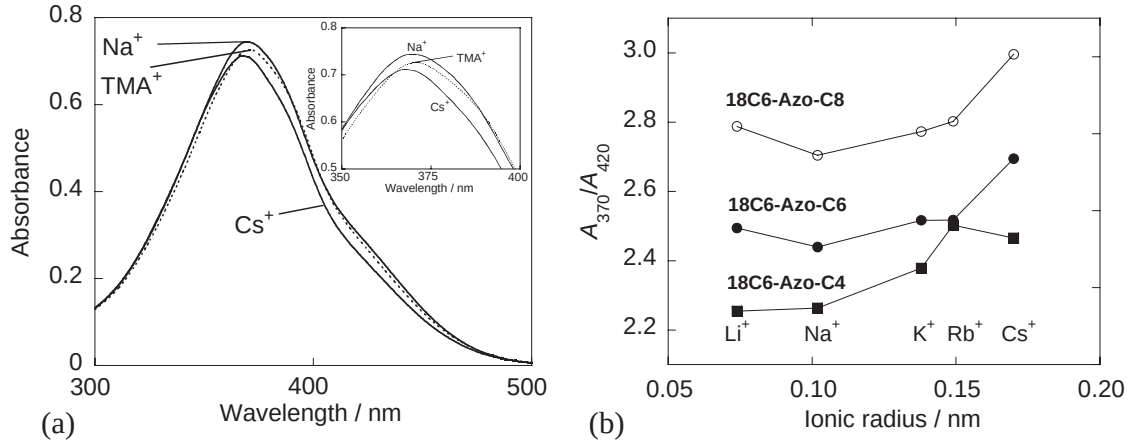

Figure 3. (a) UV–vis absorption changes of 18C6–Azo–C6 on addition of 400 mM chloride salt of alkali metal ions. (b) Response of 18C6–Azo–C*n* ($n = 4$, 6, and 8) for each alkali metal ion. [MCl] = 400 mM ($M^+ = Li^+$, Na^+, K^+, Rb^+, and Cs^+), [18C6–Azo–C*n*] = 3.0 mM.

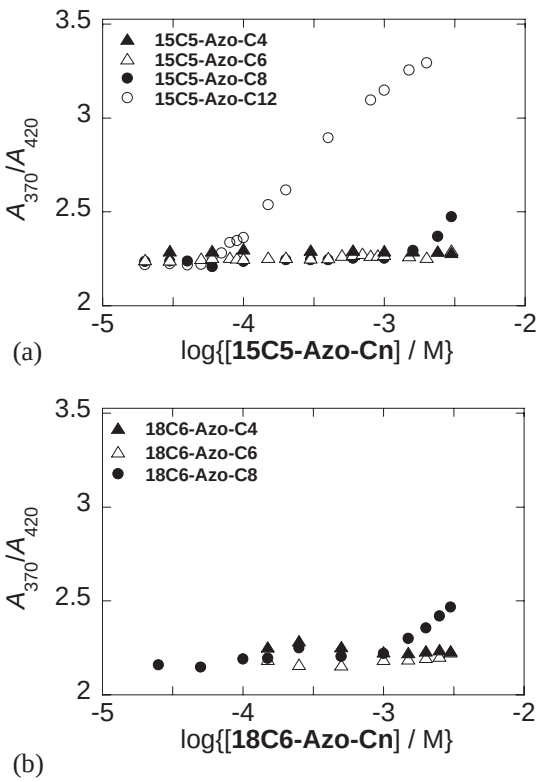

Figure 4. Concentration dependence of A_{370}/A_{420} for some azoprobes. (a) 15C5–Azo–C*n* ($n = 4$, 6, 8, and 12). (b) 18C6–Azo–C*n* ($n = 4$, 6, and 8).

phobic interaction of long alkyl chain spacers. The addition of KCl induced a blue shift of λ_{max} and the A_{370}/A_{420} values were further increased by the formation of H-aggregate dimers. The extent of peak shift and the changes in A_{370}/A_{420} values upon the addition of Cs^+ were smaller for 18C6–Azo–C*n* than for 15C5–Azo–C*n*, indicating weaker dipole–dipole interaction between phenylazo moieties because the distance between phenylazo moieties in H-aggregate dimers is longer as the radius of Cs^+ is larger than that of K^+. As a result, an azoprobe having longer alkyl spacer is advantageous in terms of sensitivity, but exhibits too much aggregation to suppress binding with alkali metal ion, resulting in loss of ion selectivity.

Table 1. Changes in Maximum Wavelength (λ_{max}) and A_{370}/A_{420} on Addition of KCl to 15C5–Azo–C*n*, or CsCl to 18C6–Azo–C*n*[a)]

n	15C5–Azo–C*n* (+KCl)		18C6–Azo–C*n* (+CsCl)	
	λ_{max}/nm	A_{370}/A_{420}	λ_{max}/nm	A_{370}/A_{420}
4	370 (366)	2.3 (2.6)	370 (368.5)	2.3 (2.5)
6	370 (366)	2.5 (3.0)	370 (367.5)	2.5 (2.7)
8	368.5 (365.5)	2.9 (3.3)	370.5 (367.5)	2.8 (3.0)
12	367 (366)	3.6 (3.8)	—	—

a) [azoprobe] = 3.0 mM, ionic strength was 400 mM (adjusted with TMACl).

Evaluation of Binding Efficiency. To evaluate the binding efficiency of the azoprobes with alkali metal ions, the effect of metal ion concentration on the absorbance changes in the UV–vis spectra was examined. Assuming that the change in absorbance is induced by 2:1 complex formation between the azoprobe (L) and the metal ion (M^+) as shown in eq 1, the relationship between absorbance (Abs.) and concentration of alkali metal ion ($[M^+]$; $[M^+] \approx [M]_t$) is expressed by eq 3:

$$M^+ + 2L \rightleftharpoons ML_2 \quad (1)$$

$$K_{ML2} = \frac{[ML_2]}{[M^+][L]^2} \quad (2)$$

$$\text{Abs.} = \frac{l}{4K_{ML2}[M^+]}\left(B\varepsilon_L + \frac{B^2\varepsilon_{ML2}}{4}\right)$$

$$B = -1 + \sqrt{1 + 8K_{ML2}[M^+][L]_t} \quad (3)$$

where K_{ML2} is an apparent 2:1 binding constant of azoprobe for alkali metal ion, $[L]_t$ is the total concentration of 15C5–Azo–C*n*, l is the optical path length (0.01 cm), and ε_L and ε_{ML2} represent the molar absorptivity of L and ML_2, respectively. It should be noted that azoprobes having long alkyl spacers, such as 15C5–Azo–C8, 15C5–Azo–C12, and 18C6–Azo–C8, showed aggregation behavior ($A_{370}/A_{420} > 2.3$) before the addition of alkali metal ion. Thus, the binding equilibria became more complicated, making the determination

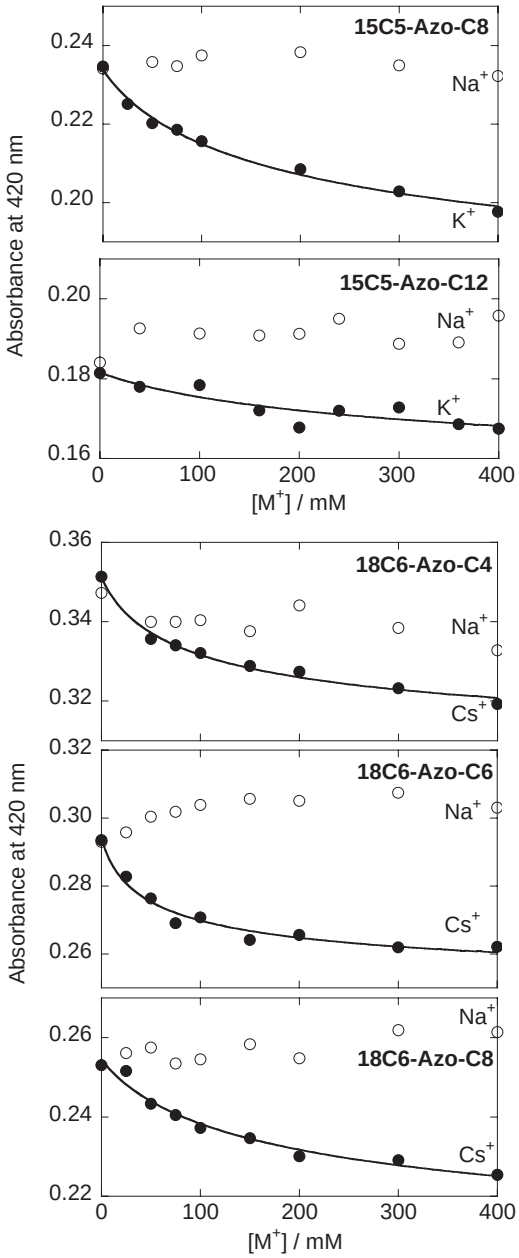

Figure 5. UV–vis absorbance changes at 420 nm of 15C5–Azo–C*n* ($n = 8$ and 12) and 18C6–Azo–C*n* ($n = 4$, 6, and 8) as a function of alkali metal ion concentration. Ionic strength is adjusted to 400 mM by the addition of TMACl.

of precise binding constant difficult. In this study, the apparent K_{ML2} values of azoprobe for alkali metal ion were assessed as an index under the same experimental conditions. The absorbance changes at 420 nm as a function of $[M^+]$ for 15C5–Azo–C*n* are depicted in Figure 5, where the ionic strength is kept constant at 400 mM by adding TMACl. For K^+, the observed results were well fitted with eq 3 (solid lines in Figure 5) using a nonlinear least-squares program, and K_{ML2} were determined (Table 2). For Na^+, the absorbance changes were small, and thus the K_{ML2} values could not be determined from eq 3. It is evident that 15C5–Azo–C6 has the highest K^+/Na^+ selectivity and the largest binding efficiency for K^+. Similarly, curve fitting analysis was carried out for 18C6–Azo–C*n* with

Table 2. Indices of Binding Efficiency between Alkali Metal Ion and Azoprobe (K_{ML2}) of 15C5–Azo–C*n* on Addition of K^+ (Left) and 18C6–Azo–C*n* on Addition of Cs^+ (Right)

n	K_{ML2} (10^3 M^{-2})	
	15C5–Azo–C*n* for K^+	18C6–Azo–C*n* for Cs^+
4	0.5 ± 0.1[a)]	1.9 ± 0.5
6	2.5 ± 0.4[a)]	3.6 ± 1.3
8	0.9 ± 0.2	0.9 ± 0.4
12	0.5 ± 0.7	

a) Quoted from Ref. 9.

CsCl or NaCl and the results are shown in Figure 5. The observed K_{ML2} values are also listed in Table 2. The results revealed that 18C6–Azo–C6 exhibited better Cs^+/Na^+ selectivity than 18C6–Azo–C4 or –C8. The binding constants of 18C6–Azo–C*n* were similar to those of 15C5–Azo–C*n*, indicating that the binding ability is related to the nature of the aggregation and not to the ring size of crown ether.

Conclusion

We synthesized amphiphilic crown ether azoprobes having various alkyl spacer lengths and crown ether ring sizes (15C5–Azo–C*n*; $n = 4$, 6, 8, and 12 and 18C6–Azo–C*n*; $n = 4$, 6, and 8). The effects of alkyl spacer length and crown ether ring size on the binding selectivity and the binding efficiency for alkali metal ions in water were evaluated. The azoprobes exhibited a hypsochromic shift due to self-assembly triggered by K^+ binding (for 15C5–Azo–C*n*) or Cs^+ binding (for 18C6–Azo–C*n*). The alkyl spacer length for optimum K^+ selectivity was determined to be $n = 6$ for 15C5–Azo–C*n*. Due to the long alkyl spacer, 15C5–Azo–C12 formed aggregates in which the TMA units were located outside the aggregates. Azoprobes having long alkyl spacers are advantageous in terms of sensitivity, although too much aggregation interferes with sandwich complex formation with alkali metal ions, resulting in loss of ion selectivity. For 18C6–Azo–C*n*, Cs^+ selective response was also dependent on the alkyl spacer length. Improved response to Cs^+ was noted for 18C6–Azo–C6 and 18C6–Azo–C8.

This work was supported by a Grant-in-Aid (No. 18350043) from the Ministry of Education, Culture, Sports, Science and Technology, Japan and the Toray Scientific Foundation.

Supporting Information

Detailed results are available in Supporting Information (Figure S1). This material is available free of charge on the Web at: http://www.csj.jp/journals/bcsj/.

References

1 a) W.-S. Xia, R. H. Schmehl, C.-J. Li, *J. Am. Chem. Soc.* **1999**, *121*, 5599. b) M. Licchelli, A. O. Biroli, A. Poggi, *Org. Lett.* **2004**, *8*, 915.

2 a) S.-Y. Lin, S.-W. Liu, C.-M. Lin, C.-H. Chen, *Anal. Chem.* **2002**, *74*, 330. b) L. Wang, X. Liu, X. Hu, S. Song, C. Fan, *Chem. Commun.* **2006**, 3780. c) C.-Y. Chen, C.-T. Cheng, C.-W. Lai, P.-W. Wu, K.-C. Wu, P.-T. Chou, Y.-H. Chou, H.-T.

Chiu, *Chem. Commun.* **2006**, 263.

3 a) K. Fujimoto, Y. Muto, M. Inouye, *Chem. Commun.* **2005**, 4780. b) H. Ueyama, M. Takagi, S. Takenaka, *J. Am. Chem. Soc.* **2002**, *124*, 14286.

4 a) A. Yamauchi, T. Hayashita, A. Kato, S. Nishizawa, M. Watanabe, N. Teramae, *Anal. Chem.* **2000**, *72*, 5841. b) T. Hayashita, A. Yamauchi, A.-J. Tong, J. C. Lee, B. D. Smith, N. Teramae, *J. Inclusion Phenom. Macrocyclic Chem.* **2004**, *50*, 87. c) T. Hayashita, D. Qing, M. Minagawa, J. C. Lee, C. H. Ku, N. Teramae, *Chem. Commun.* **2003**, 2160.

5 J. N. Israelachvili, *Intermolecular and Surface Forces with Applications to Colloidal and Biological Systems*, McGraw-Hill, N.Y., **1991**.

6 F. Sato, K. Sakamoto, W. Umemoto, T. Hashimoto, T. Hayashita, *Chem. Lett.* **2007**, *36*, 880.

7 W.-S. Xia, R. H. Schmehl, C.-J. Li, *Chem. Commun.* **2000**, 695.

8 a) A. Yamauchi, T. Hayashita, A. Kato, N. Teramae, *Bull. Chem. Soc. Jpn.* **2002**, *75*, 1527. b) J.-S. Yang, C.-Y. Hwang, M.-Y. Chen, *Tetrahedron Lett.* **2007**, *48*, 3097.

9 N. Yoshida, H. Yamaguchi, T. Iwao, M. Higashi, *J. Chem. Soc., Perkin Trans. 2* **1999**, 379.

10 M. Kasha, H. R. Rawls, M. A. El-Bayoumi, *Pure Appl. Chem.* **1965**, *11*, 371.

11 R. M. Izatt, K. Pawlak, J. S. Bradshaw, R. L. Bruening, *Chem. Rev.* **1991**, *91*, 1721.

12 T. Kunitake, Y. Okahata, *J. Am. Chem. Soc.* **1980**, *102*, 549.

13 T. Kunitake, Y. Okahata, *J. Am. Chem. Soc.* **1977**, *99*, 3860.

14 Y. Kikuchi, K. Haramoto, S. Mochizuki, A. Wakisaka, *Chem. Lett.* **2004**, *33*, 214.